Int. J. Solids Structures Vol. 25, No. 6, pp. 609–619, 1989
Printed in Great Britain.

0020–7683/89 $3.00 + .00

A COMPARISON OF MEASURED AND PREDICTED SECOND- AND THIRD-ORDER ELASTIC CONSTANTS OF A TEXTURED AGGREGATE

GEORGE C. JOHNSON and WILLIAM C. SPRINGER
Department of Mechanical Engineering, University of California, Berkeley, CA 94720, U.S.A.

(*Received* 10 *July* 1987; *in revised form* 12 *October* 1988)

Abstract—The elastic nonlinearity which leads to the acoustoelastic effect involves the introduction of a strain energy function which is cubic in the strain and thus requires both second- and third-order elastic constants. The complete set of nine second-order and 20 third-order elastic constants for a rolled plate of 7039-T64 aluminum exhibiting orthotropic texture has been experimentally determined from ultrasonic measurements and is compared to the constants predicted on the basis of x-ray determination of the texture. The predictions are in reasonable agreement with the measurements, but demonstrate the sensitivity of the x-ray technique to the single crystal constants used in the evaluation. It is also shown that the use of cubical samples for ultrasonic evaluation of the third-order constants can lead to erroneous results.

INTRODUCTION

Acoustoelasticity is a nondestructive technique for the evaluation of active and residual stresses within a structural component. With this technique being applied more widely in the field, as well as being investigated in the laboratory, it has become clear that the anisotropy of the material involved plays a significant role in determining the ultimate utility of the technique in its usual form (Pao *et al.*, 1984).

The acoustoelastic technique is based on the observation that the speeds at which various elastic waves propagate through a material depend not only on the material's elastic stiffness but also on the amount of deformation or stress to which it is subjected. In the usual approach, if a material's elastic and acoustoelastic constants are known, and if sufficiently precise measurements of velocity are made, the stress may be evaluated. We note, however, that an alternative approach in which the elastic constants do not need to be known has also been suggested (Lee *et al.*, 1986; Man and Lu, 1987). The consideration of only a material's second-order elastic constants (SOEC) does not explain the observed variation of wave speed. When third-order elastic constants (TOEC) are taken into account, the relationship between applied stress and the relative velocity change of the wave may be quantitatively analyzed.

In the simplest case of an isotropic material, applying a plane state of stress causes the velocities of waves propagating in the direction normal to the plane to vary linearly with the magnitude of the stress. For the longitudinal wave, the velocity change is proportional to the sum of the principal stresses. The changes in the shear wave velocities are related to the stress in a more complicated way, but the difference in shear wave speeds, called birefringence, is proportional to the difference of the principal stresses.

Texture may be defined as the preferred crystalline orientation which leads to a material's macroscopic anisotropy. The primary effect of texture on acoustoelasticity is that the textured material exhibits birefringence in its unstressed state. This means that the measured difference in shear wave speeds is no longer proportional to the difference in principal stresses. Texture also has the less widely recognized effect that the acoustoelastic constants themselves can display substantial anisotropy.

In the following sections, we compare the predicted and measured elastic constants of a rolled aluminum plate. We first introduce the acoustoelastic equations. Then we give a brief summary of the work which allows a material's elastic and acoustoelastic response to be evaluated from a knowledge of the material parameters and orientation distribution of the constituent crystals. This is followed by an experimental investigation into the utility of

this analysis for a particular aluminum alloy (7039-T64). The complete sets of experimentally obtained and predicted constants are presented for the material.

THEORETICAL ANALYSIS

1. *Acoustoelasticity*

The equations governing acoustoelasticity (see Pao *et al.*, 1984, for example) are based on the behavior of an infinitesimal disturbance superposed on a material subject to a finite deformation. The material under consideration must have a nonlinear stress-strain relation to account for the observed variation in elastic wave velocity with applied stress. This is accomplished by allowing the expression for the material's stored energy to be a cubic function in the strain, thus requiring the usual set of second-order (Lamé) constants and a set of third-order (Murnaghan) constants for the complete characterization of the material.

In describing the acoustoelastic response, it is convenient to introduce three configurations of the body: the undeformed reference configuration κ_0 in which a material particle is located by the position vector $\mathbf{X}$; the homogeneously deformed configuration κ in the absence of the superposed disturbance, in which the particle is located by the position vector $\mathbf{x}$; and the current configuration κ' in which the particle is located by the position vector $\mathbf{x}'$. Given that κ' differs from κ by an infinitesimal deformation, we write

$$\mathbf{x}' = \mathbf{x} + \mathbf{u} \tag{1}$$

where $\mathbf{u}$ is the displacement vector associated with the propagating wave. The deformation gradient in κ' is related to that in κ as

$$F'_{iA} = \frac{\partial x'_i}{\partial X_A} = \frac{\partial x_j}{\partial X_A}\left(\delta_{ij} + \frac{\partial u_i}{\partial x_j}\right) = F_{jA}(\delta_{ij} + u_{i,j}). \tag{2}$$

Similarly, the Lagrangian strains in κ' and κ are related as

$$E'_{AB} = \tfrac{1}{2}(F'_{iA}F'_{iB} - \delta_{AB}) = E_{AB} + F_{iA}F_{jB}e_{ij} \tag{3}$$

where e_{ij} is the increment in strain caused by $\mathbf{u}$ as seen from κ. Since $\mathbf{u}$ is taken to be infinitesimal, we let

$$e_{ij} = \tfrac{1}{2}(u_{i,j} + u_{j,i}). \tag{4}$$

The constitutive relation between stress and strain in κ_0 is introduced through the strain energy function Φ as

$$\rho_0\Phi = \tfrac{1}{2}C_{ABCD}E_{AB}E_{CD} + \tfrac{1}{2}C_{ABCDEF}E_{AB}E_{CD}E_{EF} \tag{5}$$

where ρ_0 is the mass density in κ_0 and the coefficients C_{ABCD} and C_{ABCDEF} are the material's second- and third-order elastic constants, respectively. The constitutive relation for the Cauchy stress T_{ij} is given in terms of Φ as

$$T_{ij} = \frac{1}{J}F_{iA}F_{jB}\frac{\partial}{\partial E_{AB}}(\rho_0\Phi) \tag{6}$$

where $J = \det \mathbf{F} = \rho_0/\rho$ and ρ is the mass density in κ. An entirely analogous expression holds for the stress T'_{ij} in κ' if $\mathbf{E}$ and $\mathbf{F}$ are replaced by $\mathbf{E}'$ and $\mathbf{F}'$ in eqns (5) and (6).

The acoustoelastic response is evaluated by considering the equations which govern the motion κ'. In terms of the Cauchy stress these equations may be written as

$$\frac{\partial T'_{ij}}{\partial x'_i} = \rho' \ddot{u}_j \tag{7}$$

where body forces have been neglected. Linearizing eqn (7) in **u** and its gradients leads to the partial differential equation in **u** of the form

$$(\hat{C}_{ijkl} + T_{il}\delta_{jk})u_{k,il} = \rho \ddot{u}_j \tag{8}$$

where what may be called the "current stiffness" $\hat{C}_{ijkl}$ is

$$\hat{C}_{ijkl} = \frac{\rho}{\rho_0} F_{iA} F_{jB} F_{kC} F_{lD} \frac{\partial^2(\rho_0 \Phi)}{\partial E_{AB} \partial E_{CD}}. \tag{9}$$

By using eqn (5), we may rewrite eqn (9) as

$$\hat{C}_{ijkl} = \frac{\rho}{\rho_0} F_{iA} F_{jB} F_{kC} F_{lD} (C_{ABCD} + C_{ABCDEF} E_{EF}). \tag{10}$$

If **u** is taken to have the form of a plane wave,

$$u_i = U_i \, e^{jk(\mathbf{n} \cdot \mathbf{x} - Vt)} \tag{11}$$

where U_i is the amplitude, k the wave number, **n** the unit vector in the direction of propagation, and V the wave speed, then eqn (8) becomes

$$[(\hat{C}_{ijkl} + T_{il}\delta_{jk})n_i n_l - \rho V^2 \delta_{jk}] U_k = 0. \tag{12}$$

Equation (12) thus represents an eigenvalue problem from which V can be evaluated for given propagation direction **n**, with the eigenvector U_k being the polarization.

Now, if the dependence of V on stress is measured for waves propagating and polarized in particular directions, the solutions of eqn (12) can be used to evaluate the elastic constants of eqn (5). Some combinations of these constants are commonly evaluated experimentally from measurements of the wave velocity in the undeformed material and changes of velocity during the application of known uniaxial stress. The task of completely characterizing the acoustoelastic behavior of a rolled metal is, however, formidable since there are nine independent SOEC and 20 independent TOEC which must be determined. Indeed the only such characterization for an orthorhombic material was presented by Haussühl and Chmielewski (1981) for calcium formate.

2. *Orientation distribution function*

As an alternative to the ultrasonic characterization of the material, a method for estimating an aggregate's elastic constants from knowledge of the elastic constants of a single crystal and the orientation distribution of crystallites in the aggregate has been proposed by Johnson (1985). The orientation of a particular grain in the aggregate is given by the Euler angles Θ, ψ, and φ. The orientation distribution function (ODF) for all of the grains is a function whose integral over a range of Euler angles gives the probability that any grain will be within that range of possible orientations. In this work the material texture is assumed to be homogeneous so that the ODF is independent of position within the material.

As described in Roe (1965, 1966), there exists an harmonic expression for the distribution function involving the Euler angles and real texture coefficients W_{lmn} which must obey certain interdependencies in order to satisfy the assumed cubic crystal and orthorhombic aggregate symmetries (Johnson, 1985). Under the assumptions used in Johnson (1985), the aggregate's SOEC and TOEC introduced in eqn (5) are related to the crystallites' elastic constants through the ODF. This result is given in detail in Johnson (1985) for the

case of cubic crystal and orthorhombic specimen symmetries and may be summarized in the form

$$C_{ABCD} = C^{*}_{ABCD} + C^{**}_{ABCD}$$
$$C_{ABCDEF} = C^{*}_{ABCDEF} + C^{**}_{ABCDEF}. \tag{13}$$

The terms C^{*}_{ABCD} and C^{*}_{ABCDEF} are the crystallite stiffnesses referred to the grain's principal symmetry axes. The C^{**}_{ABCD} depend on a single combination of the crystal's SOEC and on three texture coefficients referred to above: W_{400}, W_{420}, and W_{440}. The C^{**}_{ABCDEF} depend on three combinations of the crystal's TOEC and on a total of seven texture coefficients: the previous three, W_{600}, W_{620}, W_{640}, and W_{660}. It is of interest to note that the combinations of SOEC and TOEC which enter C^{**}_{ABCD} and C^{**}_{ABCDEF} are measures of the crystalline anisotropy since these combinations vanish for an isotropic material.

EXPERIMENTAL PROCEDURES

1. *Ultrasonic technique*

The ultrasonic measurements were of two basic types: measurements of absolute velocity in the unstressed material (which led to the SOEC) and measurements of relative velocity change under the application of uniaxial stress (which led to the TOEC). The double-pulse echo system described by Ilić *et al.* (1979), and which operates in a phase-locked loop, was used for both types of measurements. In this system, the frequency of an ultrasonic carrier signal is varied to maintain a constant phase difference between reflections from the front and back faces of a material specimen. During the application of stress, the frequency change can be related to the velocity change through a measurement of the change in path length. Thus, the change in frequency measured with this system is just the change in "natural velocity" defined by Thurston and Brugger (1964).

Six of the nine SOEC may be obtained by measuring the velocities of pure mode waves propagating in the X_1, X_2, or X_3 directions in the unstressed material. We have chosen X_1 to correspond to the plate's rolling direction (RD), X_2 to the direction normal to the plate (ND), and X_3 to the plate's transverse direction (TD). The remaining three SOEC may be determined from the velocities of either quasilongitudinal or quasishear waves propagating in off-axis directions. Expressions for these constants may be obtained from the characteristic equation (12) under the no-stress condition.

Evaluation of the TOEC requires that the relative change in wave speed be measured during the application of a known stress. Eighteen of the 20 independent TOEC can be determined by measuring the changes in the speeds of the pure mode waves propagating along the principal directions of anisotropy with loading along one of the principal directions (Springer, 1986). Specifically, let D^{A}_{BC} be the relative velocity change of a wave propagating along X_B with particle motion along X_C and with uniaxial stress applied along X_A. By solving for the velocities in the characteristic equation which results from eqn (12), D^{A}_{BC} can be expressed as

$$D^{A}_{BC} = \sum_{R=1}^{3} \left(\frac{C_{RRBCBC} + \delta_{AB}\delta_{BC}C_{RRBB}}{2C_{BCBC}} + \delta_{RB} + \delta_{RC} \right) E^{(A)}_{RR} \tag{14}$$

where $E^{(A)}_{RR}$ is the normal strain in the X_R direction associated with the stress acting along X_A. The only summation in eqn (14) is that which explicitly involves R. For a particular wave type (that is, for particular values of B and C), eqn (14) gives three equations associated with loading along the X_1, X_2, and X_3 directions. From these, the third-order constants C_{11BCBC}, C_{22BCBC}, and C_{33BCBC} can be calculated.

Two TOEC, C_{112233} and C_{233112}, do not appear in any of eqn (14). Their evaluation requires either loading or wave propagation in a direction other than a principal direction. To obtain expressions involving C_{112233}, a wave propagating in the (1, 1, 0) direction with

loading in the X_3 direction is used. The explicit expression for this relative velocity change $D_{L,s}$ is found to be

$$D_{L,s} = \frac{A \pm (B + 4FC_{112233})}{4(G+H)} E_{33} \tag{15}$$

where the coefficients A, B, F, G, and H contain previously determined SOEC and TOEC. The "+" equation applies to the quasilongitudinal wave, while the "−" equation applies to the quasishear wave polarized in the 1–2 plane. To obtain a relation that involves C_{233112}, we consider loading in the (1, 0, 1) direction. A shear wave propagates in the (1, 0, −1) direction and is polarized in the X_2 direction. From this condition we obtain the expression for the relative velocity

$$D_{456} = JE_{11} + KE_{22} + LE_{33} + (M + 2C_{233112})E_{13} \tag{16}$$

where J, K, L, and M are expressions containing previously determined SOEC and TOEC. We note that this expression for C_{233112} is the only one in which a shear strain, E_{13}, appears.

Because of the need to have loads applied and waves propagate in a variety of directions, several different samples were required. One of the loading conditions involved uniaxial stress applied in the plate's ND (X_2 direction). The thickness of the plate (nominally 25 mm) required that this stress by applied in compression since this dimension is too small for a tension specimen. Thus, compression tests were selected for all loading conditions.

Initially, three cubical samples were thought to be sufficient: one which would allow loading and wave propagation in any of the principal directions, one which could be loaded in the X_3 direction with wave propagation possible in the directions (1, ±1, 0), and one which could be loaded in the direction (1, 0, −1) with wave propagation possible in the directions (1, 0, 1) and (0, 1, 0). In order to allow waves to propagate along the direction of loading, a special compression grip in which the ultrasonic transducer could be mounted was designed and built. The acoustoelastic response observed on the cubical sample did not, however, correspond to that observed during uniaxial tension on a standard "dog-bone" tension specimen of the same material. Rather, the results from the compression tests were roughly 30% lower than those from the tension tests. A more extensive examination of this situation indicated that the stress state in the cubical sample under the applied compressive load was not the assumed uniform state, but one in which the bulk of the load was carried along the outer edges of the cube.

An experimental investigation of this result was performed on a sample of 2024-T351 aluminum with square cross section. Measurements of acoustoelastic response were made as the length of the sample was reduced. The initial sample dimensions were 25 mm in each of the ND and TD, and 170 mm in the RD. The acoustoelastic constant (relative frequency change per unit of applied stress) was determined for the longitudinal waves with the transducer placed in the central region of the sample. Then the block was shortened by removing equal amounts of material from the ends and the acoustoelastic constant was remeasured. This process was repeated until a cubical sample was obtained. To allow the results to be generalized to other cross-sections, the data are presented in Fig. 1 as acoustoelastic constant vs slenderness ratio (specimen length divided by radius of gyration). The measured acoustoelastic constant varies by only 2% for slenderness ratios above 8 and then falls off dramatically for slenderness ratios less than 8. The acoustoelastic constant for the cubical sample is 24% below that for the original sample.

Therefore, three separate samples were required for the principal direction tests to allow specimen lengths in the loading directions to be sufficient to provide a uniform stress state. All the samples actually used in the evaluation of the TOEC had a minimum slenderness ratio of 12. Each specimen had faces machined parallel in conformance with ASTM standards for compression testing and then sanded smooth.

In order to achieve the necessary slenderness ratio for the case of loading in the ND, a composite sample consisting of three sections glued together with a structural epoxy

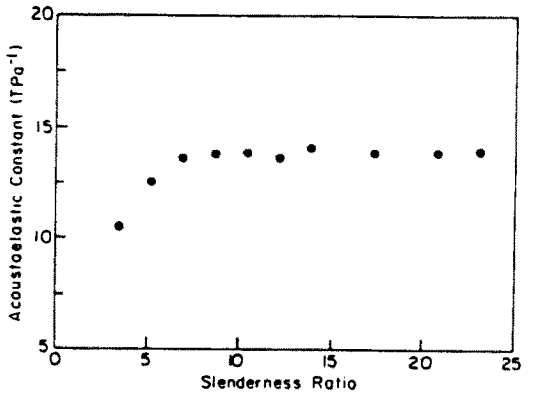

Fig. 1. Acoustoelastic constant vs slenderness ratio for 2024-T351 aluminum.

adhesive was used. A test was conducted on a well characterized sample of 2024-T351 aluminum in which a section was cut out and then glued back in. The remeasured response was in agreement with the original response, thus validating our procedure. As a final verification of our method, we compared the acoustoelastic responses of a long compression sample and a standard tension specimen. Two such tests are shown in Fig. 2 for loading in the RD with longitudinal waves propagating in the ND and TD. The differences between the results for tension and compression are within 5% in each case.

2. *x-Ray measurements*

The first step in the prediction of elastic constants from x-ray diffraction studies is to obtain pole figures. For each pole figure, x-rays from a copper source impinge upon a flat sample of the subject aluminum at the Bragg angle corresponding to the {222}, {220}, {200}, or {311} plane of interest. The intensity of the reflected x-rays is measured and stored as the sample is rotated through a spiral pattern. To first approximation, the intensity of diffracted x-rays at any given orientation is proportional to the number of crystallites that have the specific plane of interest aligned normal to that orientation. Plotting these intensities on a two-dimensional projection creates the pole figure for that plane. This process yields an incomplete pole figure since accurate measurements cannot be made beyond a tilt angle of around 80 degrees.

Three samples were prepared from the aluminum plate such that the major surfaces of the samples were perpendicular to the RD, ND, and TD. The surfaces of the specimens were polished to prevent machining damage from affecting the data. It is possible to construct one complete pole figure from measurements on three samples, but this was not needed. Rather, the three sets of measured pole figures were "inverted" independently to

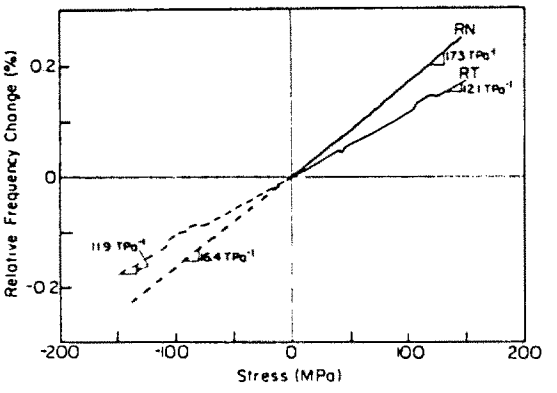

Fig. 2. Relative frequency change vs applied stress for 2024-T351 aluminum in tension and compression in the RD. Second letter of the label denotes propagation direction of the longitudinal wave.

obtain the three sets of ODF coefficients using a series of programs based on algorithms by Pospiech and Jura (1974).

RESULTS

Pole figures were measured for the {222}, {200}, {220}, and {311} crystallographic planes. The ODF coefficients for $l \leqslant 22$ were evaluated for each sample orientation by the "inversion" of the four pole figures. As a check, the coefficients were used to reconstruct the individual pole figures. The experimental and reconstructed pole figures for the {222} plane are shown in Figs (3a) and (b), respectively, and those for the {200} plane are shown in Figs 4(a) and (b). Evenly spaced contours of multiples of random distribution (m.r.d.) are noted on the pole figures. The pole figures for the {220} and {311} planes are similar. For each plane shown, the pole figures measured from the three differently oriented samples are arranged to demonstrate the consistency of the observed texture.

In all cases, the two-fold symmetry about the in-plane axes is clearly evident and the data indicate a fairly strong and consistent texture. The reconstructed pole figures agree well with the original data qualitatively, although the magnitudes of the texture peaks are substantially lower. However, the maximum m.r.d. levels for all reconstructed pole figures of any one plane are in good agreement, indicating the consistency of the experimental data. Only the first seven coefficients are used to calculate the elastic constants, and these coefficients are shown in Table 1. Note that the sets of coefficients do not display any apparent consistency from one sample to another since each set is associated with a different sample orientation.

The measured absolute velocities for the 7039-T64 alloy are listed in Table 2. The density of the material, required to evaluate the SOEC from these velocities, was determined to be 2750 ± 5 kg/m^3 with a Joly balance. Since the data in Table 2 are theoretically symmetric with respect to the interchange of propagation and polarization directions, the appropriate shear wave speeds were averaged in evaluating the SOEC.

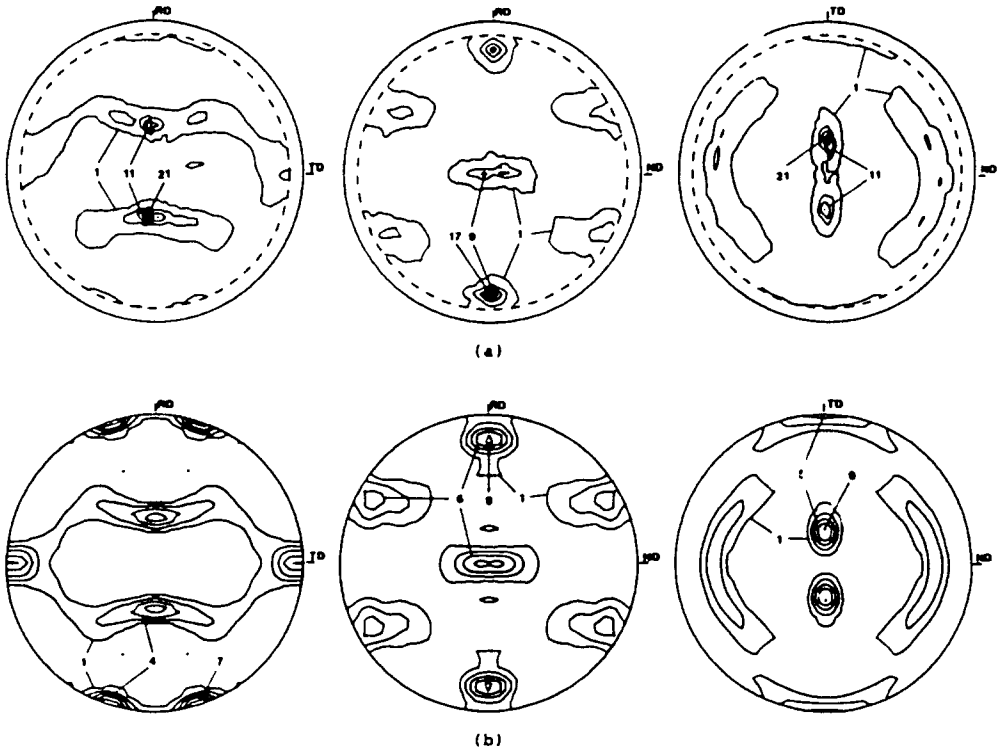

Fig. 3. Experimental (a) and reconstructed (b) pole figures for the {222} crystallographic plane of 7039-T64 aluminum. Contour values are given as m.r.d.; contours are equally spaced.

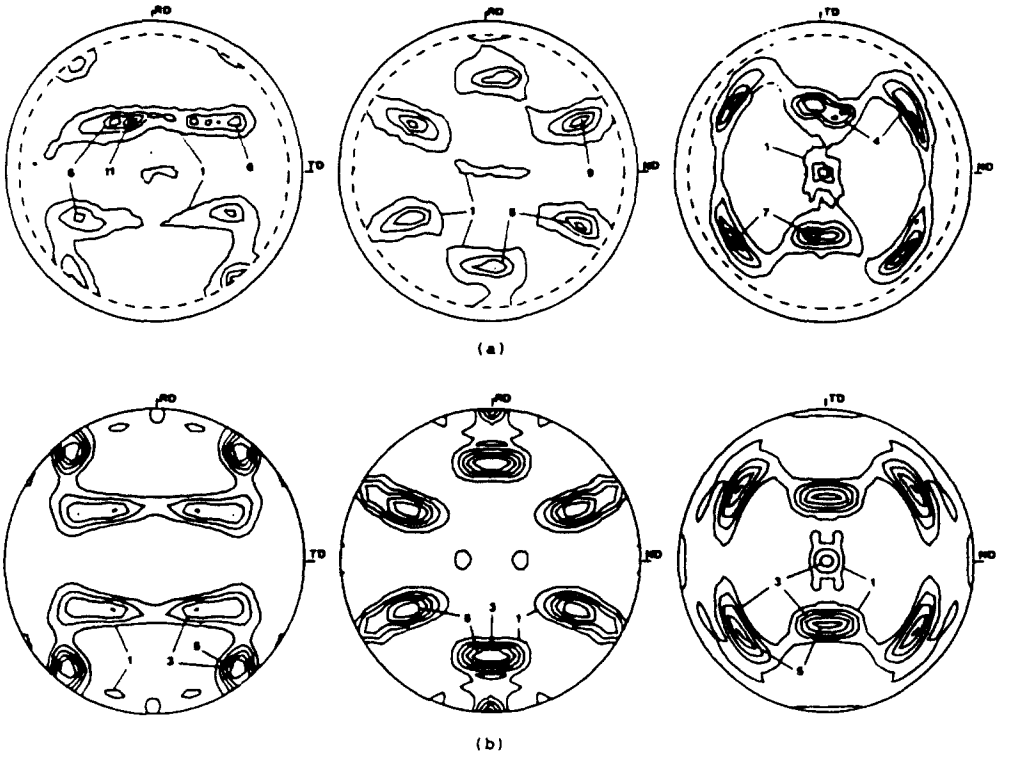

Fig. 4. Experimental (a) and reconstructed (b) pole figures for the {200} crystallographic plane of 7039-T64 aluminum. Contour values are given as m.r.d.; contours are equally spaced.

Table 1. Coefficients of the ODF, W_{lmn}, for $l \leq 6$ for 7039-T64 aluminum

	W_{lmn}		
lmn	TD	ND	RD
400	−0.0086	−0.0022	−0.0017
420	−0.00028	0.0025	0.0043
440	0.00071	−0.0071	−0.0039
600	−0.0050	0.0037	−0.0037
620	−0.0014	0.0036	−0.0055
640	0.0012	0.0026	0.0012
660	0.0089	−0.0025	−0.00057

Table 2. Experimental wave speeds in unstressed 7039-T64 aluminum

Propagation direction	Polarization direction	Velocity (m/s) (± 12 m/s)
1	1	6322
1	2	3127
1	3	3063
2	1	3119
2	2	6294
2	3	3074
3	1	3060
3	2	3098
3	3	6336
(1, 1, 0)	(1, 1, 0)	6308
(1, 0, 1)	(1, 0, 1)	6295
(0, 1, 1)	(0, 1, 1)	6291

Table 3. Experimental values of the slope of relative frequency change vs stress curves in 7039-T64 aluminum

Propagation direction	Polarization direction	Loading direction	Slope (TPa^{-1})	Uncertainty (TPa^{-1})
1	1	1	−59.7	1.5
1	1	2	9.66	0.15
1	1	3	15.6	0.3
2	2	1	16.7	0.1
2	2	2	−68.2	1.5
2	2	3	13.2	0.1
3	3	1	12.3	0.15
3	3	2	14.5	0.1
3	3	3	−66.4	1.3
3	2	1	14.6	0.3
2	3	1	14.1	0.3
3	2	2	−26.8	0.3
2	3	3	−24.2	0.4
3	1	1	−20.4	0.15
1	3	2	15.8	0.3
3	1	2	14.7	0.25
1	3	3	−33.9	0.3
2	1	1	−41.2	0.3
1	2	2	−9.8	0.3
1	2	3	16.5	0.4
2	1	3	16.3	0.9
(1, 0, 1)	2	(1, 0, −1)	2.47	0.25
(1, 1, 0)	(1, 1, 0)	3	15.7	0.15
(1, 1, 0)	(1, −1, 0)	3	11.8	0.2

The experimentally determined acoustoelastic constants, given as relative frequency change per unit applied stress, are listed in Table 3. These values are the slopes of the linear least squares fits to the actual data points gathered. In Fig. 5 we show a set of such data for the pure mode longitudinal waves propagating perpendicular to the direction of loading. The labels on the curves in this figure give the loading direction followed by the propagation direction. We note that for an isotropic material all these curves would be identical.

Table 4 contains the SOEC, and Table 5 the TOEC, evaluated by the ultrasonic and x-ray techniques. For the method involving the ODF coefficients, we used single crystal data at 298 K from two sources: Thomas (1968) and Sarma and Reddy (1972). These elastic constants are presented in groups within which all entries would have the same value for an isotropic material. The extent to which the values vary within a particular group is thus one indication of the degree of anisotropy exhibited by the aggregate. The constants

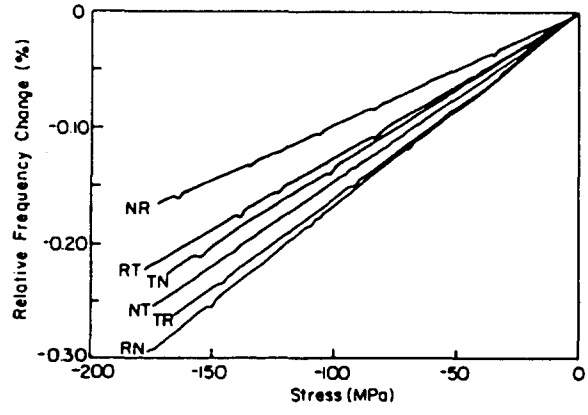

Fig. 5. Examples of relative frequency change vs applied stress curves for longitudinal waves in 7039-T64 aluminum. First letter of the label denotes the loading direction, second letter denotes wave propagation direction.

Table 4. Ultrasonic and x-ray estimates of SOEC of 7039-T64 aluminum given in GPa

	C_{ABCD} (GPa)					
ABCD	Ultrasonic	Uncertainty (%)	x-Ray (Thomas)	Uncertainty (%)	x-Ray (Sarma and Reddy)	Uncertainty (%)
1111	109.9	0.5	111.3	0.2	111.3	0.3
2222	108.9	0.5	111.3	0.3	111.1	0.1
3333	110.4	0.5	112.1	0.2	112.0	0.2
1122	56.6	2.0	58.5	0.1	58.6	0.2
1133	56.9	2.0	57.7	0.3	57.6	0.4
2233	56.6	2.0	57.7	0.3	57.9	0.1
2323	26.2	0.5	25.6	1.1	25.8	0.3
3131	25.8	0.5	25.6	1.1	25.5	0.8
1212	26.8	0.5	26.4	0.3	26.5	0.4

determined from the x-ray analyses are averages of the results from the three sample orientations. The percent variation noted in Table 4 for an ultrasonic value is the standard deviation calculated from the least squares fit to the ultrasonic data. The variation for an x-ray value is the standard deviation among the three values of each constant obtained from the three sets of differently oriented ODF coefficients.

In Table 4 it can be seen that the SOEC from the two sets of x-ray values agree well with each other and generally agree with the ultrasonic results. The results in Table 5 indicate that the third-order response predicted from the ODF coefficients is generally more anisotropic than that measured ultrasonically. That is, within each group there is more variation among the x-ray values than among the ultrasonic values. Further, both techniques indicate that this material is only slightly anisotropic in its SOEC, but its TOEC display substantial anistropy. It should also be noted that while in some groups of the TOEC (C, D, and the off-principal-axis constants) there is generally good agreement between the two techniques, in others (A and B) there is rather wide variation. In group A, in fact, there is less anisotropy shown in either set of ODF-determined constants than those determined ultrasonically.

There are several possible explanations for the variation between the ultrasonic and x-ray constants. Among these, the most plausible are that the single-crystal constants used

Table 5. Ultrasonic and x-ray estimates of TOEC of 7039-T64 aluminum given in GPa

		C_{ABCDEF} (GPa)					
Group	*ABCDEF*	Ultrasonic	Uncertainty (%)	x-Ray (Thomas)	Uncertainty (%)	x-Ray (Sarma and Reddy)	Uncertainty (%)
A	111111	−1450	3	−1400	5	−1590	2
	222222	−1580		−1350	7	−1490	3.5
	333333	−1610		−1400	2	−1570	3
B	111122	−370	9	−180	25	−200	19
	111133	−300		−270	5	−350	12
	222211	−340		−250	32	−340	14
	222233	−370		−270	10	−330	8
	333311	−410		−210	20	−260	12
	333322	−380		−210	20	−270	14
C	112323	−130	4	−110	17	−150	12
	223131	−130		−120	15	−160	21
	331212	−120		−75	31	−100	29
D	113131	−280	2	−270	2	−290	3
	111212	−330		−260	10	−290	6
	222323	−290		−280	3	−320	4
	221212	−240		−250	12	−270	6
	332323	−290		−240	28	−230	6
	333131	−320		−300	26	−350	9
	112233	−65	20	−64	4	−55	5
	233112	−110	1	−96	3	−93	3

Table 6. Combinations of ultrasonic estimates of SOEC given in eqns (17) and (18) for 7039-T64 aluminum. Values are in GPa

A	B	C	$C_{AABB}-C_{ABAB}$	$C_{AAAA}-C_{BBBB}$	$C_{BBCC}-C_{AACC}$	$C_{BCBC}-C_{ACAC}$
1	2	3	29.8	1.0	−0.3	0.4
3	1	2	31.1	0.5	0.0	0.6
2	3	1	30.4	−1.5	0.3	−1.0

in the ODF-based calculations are not those of the 7039-T64 alloy and that the texture is not uniform, but instead varies through the thickness of the plate. As can be seen in Table 5, the calculated constants are extremely sensitive to the single-crystal data. The single-crystal elastic constants taken from Thomas and from Sarma and Reddy were both for aluminum of between 99.95% and 99.99% purity. The alloy we used, however, contains up to 4.5% zinc, 3.3% magnesium, 0.4% manganese, and 1% additional elements; it is reasonable to expect that the SOEC and TOEC of this alloy would differ somewhat from those of a high purity aluminum. Given the severity of the material texture, the presence of a texture gradient would tend to reduce the anisotropy in the ultrasonically determined constants. In addition, for any TOEC found by ODF analysis in group B or C, there is substantial disagreement among the three values making up the average.

Evidence that both of these factors may be involved is found by considering the relations which should exist among the aggregate's SOEC. Specifically, the SOEC derived from a homogeneous texture should be related as

$$C_{AABB}-C_{ABAB}=C^{*}_{1122}-C^{*}_{1212} \quad (A\neq B, \text{ no summation}) \tag{17}$$

and

$$C_{AAAA}-C_{BBBB}=C_{BBCC}-C_{AACC}=C_{BCBC}-C_{ACAC} \quad (A\neq B\neq C). \tag{18}$$

In Table 6 these combinations are presented for the ultrasonically measured SOEC. Since the value of $C^{*}_{1122}-C^{*}_{1212}$ is 32.1 GPa, we find that the measured data and the assumed single crystal data do not agree. Further, the results of calculating eqn (18) with the measured data as shown in Table 6 indicate inconsistency with the assumption that a single ODF governs the entire body.

REFERENCES

Haussühl, S. and Chmielewski, W. (1981). Third-order elastic constants of orthorhombic calcium formate. *Acta Cryst.* **A37**, 361–364.

Ilić, D. B., Kino, G. S. and Selfridge, A. R. (1979). Computer-controlled system for measuring two-dimensional acoustic velocity fields. *Rev. Sci. Instrum.* **50**, 1527–1533.

Johnson, G. C. (1985). Acoustoelastic response of a polycrystalline aggregate with orthotropic texture. *J. Appl. Mech.* **52**, 659–663.

Lee, S. S., Smith, J. F. and Thompson, R. B. (1986). Absolute acoustoelastic measurements of stress in textured plate with arbitrary stress orientation. In *Review of Progress in Quantitative NDE*, Vol. 5 (Edited by D. O. Thompson and D. E. Chimenti), pp. 1423–1430. Plenum Press, New York.

Man, C.-S. and Lu, W. Y. (1987). Towards an acoustoelastic theory for measurement of residual stress. *J. Elasticity* **17**, 159–182.

Pao, Y. H., Sachse, W. and Fukuoka, H. (1984). Acoustoelasticity and ultrasonic measurements of residual stress. In *Physical Acoustics*, Vol. 17 (Edited by W. P. Mason and R. N. Thurston), pp. 61–143. Academic Press, New York.

Pospiech, J. and Jura, J. (1974). Determination of the orientation distribution function from incomplete pole figures. *Z. Metallkunde* **65**, 324–330.

Roe, R. J. (1965). Description of crystallite orientation in polycrystalline materials. III. General solution to pole figures inversion. *J. Appl. Phys.* **36**, 2024–2031.

Roe, R. J. (1966). Inversion of pole figures for materials having cubic crystal symmetry. *J. Appl. Phys.* **37**, 2069–2072.

Sarma, V. P. N. and Reddy, P. J. (1972). Third-order elastic constants of aluminum. *Phys. Stat. Sol.* (*a*) **10**, 563–567.

Springer, W. C. (1986). Evaluation of second- and third-order elastic constants of rolled aluminum plate. Master's thesis, University of California, Berkeley.

Thomas, J. F., Jr (1968). Third-order elastic constants of aluminum. *Phys. Rev.* **175**, 955–962.

Thurston, R. N. and Brugger, K. (1964). Third-order elastic constants and the velocity of small amplitude elastic waves in homogeneously stressed media. *Phys. Rev.* **133**, A 1604–1610.